Photoreceptor Sensitivity and the Shot Noise of Chemical Processes

Donatella Petracchi,* Giovanni Cercignani,‡ and Sabina Lucia*

*Istituto di Biofisica del CNR, Via S. Lorenzo 26, 56127, Pisa, Italy; and ‡Dipartimento di Fisiologia e Biochimica, Via S. Maria 55, Università di Pisa, 56126 Pisa, Italy

ABSTRACT   The general modeling of dose-response curves to very low stimuli in a photosensory-effector system is critically reshaped starting from basic assumptions on the fluctuations of chemical signals inside the receptor cell, which add to those of the stimulus itself, both arising from their granular (or quantal) structure. We have shown, both through the analytical treatment of a simple kinetic scheme and by means of Monte Carlo simulations of the same, that shot noise arising from chemical transduction ("chemical shot noise") contributes considerably to the output noise of the receptor-effector system, thus affecting both the shape and the abscissa shift of dose-response curves under these conditions; the latter phenomenon has indeed been reported in *Halobacterium halobium*. After evaluating the general properties of a single-step amplifying mechanism, the effects of introducing several low-amplifying steps in cascade were investigated briefly. The results obtained were qualitatively and quantitatively at variance from those of earlier models on the same phenomenon, and the discrepancies are discussed in order to highlight the fundamental contribution of chemical shot noise to the response of any kind of sensory system to very low stimuli.

INTRODUCTION

A general feature, common to most sensory systems, is that the response at very low levels of the stimulus becomes a random event. The response may be of a different nature in different systems. For instance, it can be a bump in the potential recorded from neural cells in the *Limulus* eye (Fuortes and Yeandle, 1964) or a reversal in the motor behavior of a halobacterial cell (Spudich and Stoeckenius, 1979). In either case, when a fixed low-level stimulus is delivered several times to the sensory system, it does not always elicit the same response: at times a response appears, at other times it does not.

The first attempt at interpreting the randomness of the responses to low light stimuli was made in the early 1940s by Hecht et al. (1942). Their approach was based on the consideration that at very low light intensity the stimulation itself occurs randomly, due to the quantum nature of light.

If we deliver a flash on a cell population and an average number, α, of photons is absorbed per cell through sensory pigment molecules, the probability that a single cell actually absorbs m photons during the flash is given by

$$P(m) = \frac{\alpha^m}{m!} e^{-\alpha} \qquad (1)$$

Let l be a fixed number of photons representing a threshold of the system. Then the probability that the cell absorbs more than l photons is given by

$$P(m \geq l) = \sum_{m=1}^{\infty} \frac{\alpha^m}{m!} e^{-\alpha} = 1 - \sum_{m=0}^{l-1} \frac{\alpha^m}{m!} e^{-\alpha}. \qquad (2)$$

This represents the dose-response curve of the system. As a function of α, Eq. 2 describes a family of curves characterized by the value of l; the slope of these curves increases with increasing values of l. Moreover, the absolute sensitivity, defined as $1/\alpha_{1/2}$ (the reciprocal of the α value at which the response probability is $1/2$), also depends on l, e.g., for $l = 1$, $1/\alpha_{1/2} = 2$, whereas for $l = 2$, $1/\alpha_{1/2} = 0.5$.

In the classical approach of Hecht et al. (1942), these expressions were used to fit the dose-response curves for the human eye perception of dim light flashes. The tacit assumption was made that the noise in the response is completely due to input noise, and no other sources of noise were present in the intracellular signal processing. With this in mind, the experimental fluence-response curves can be compared with the Poisson curves in order to determine the number of activated photoreceptors required to elicit a perception.

Since then, the variability intrinsic to weak stimuli has been used widely as the basic interpretation of response variability. However, chemical signals are themselves made of particles (molecules or ions). This was explained by Borsellino and Fuortes (1968a). When elementary responses are considered, "it is essential to take into account the stochastic fluctuations of the response in addition to the fluctuations of the stimulus." We do not agree with the analytical results of these two authors (Borsellino and Fuortes, 1968a,b), which have been shown to be in error (Goldring and Lisman, 1983), but we take their view of the stochastic features of transduction processes as a basic start.

During the three decades after the publication of the Borsellino-Fuortes model, minimal emphasis has been

placed on the noise due to the chemical transmission of signals, although the presence of noise in the visual transduction pathway has been shown clearly by Lillywhite and Laughlin (1979). The noise in chemical transduction was invoked chiefly to account for the variability of latency (Borsellino and Fuortes, 1968a; Lederhofer et al., 1991), whereas the amplitude was expected to be almost fixed for systems with a tolerable amplification. Only recently the size variability of the response to single photons in the ventral photoreceptors of Limulus has been measured and related to theoretical predictions in two cognate papers (Kirkwood and Lisman, 1994; Goldring and Lisman, 1994). On the other hand, people working on vertebrate photoreceptor believe that the responses of rods to single photons are locally saturated and that the "quantum" responses in rods are surprisingly stereotyped. Thus the variability in responses to dim light flashes is believed to be basically due to the absorption of one, two, . . . , few photons (Baylor et al., 1984). The same way to treat the problem of interpreting the variability of responses to dim stimuli as due to the stimulus variability is maintained in other systems (olfactory neurons) (Menini et al., 1995), although there are no specific reasons to assume that responses are locally saturated.

Indeed, the pattern of the responses to dim stimuli can display different features, depending on whether the transduction process is linear. Saturation may not be present under most circumstances, but nonlinear steps may influence the size, latency, shape, and time distribution of output signals. A clear-cut treatment of this problem was presented by Grzywacz and Hillman (1985) as a test for linearity of photoreceptor transduction processes. Within that article, noise due to chemical steps purposely was taken into account to show that when only linear (first-order) steps are involved in transduction, each of them produces a number of molecules distributed as a "discrete exponential." A system behaving like this is called "nonmultiple-active-state linear system" (Grzywacz and Hillman, 1985), because it is assumed that chemical stages in the transduction process are catalyzed by enzymes with only one active state.

As far as we know, noise in transduction chains has never been taken into account in interpreting perceptive or behavioral fluence-response curves. Our interest in the analysis of the noise intrinsic to chemical transduction came from the available data on the dose-response curves of Halobacterium halobium, an archebacterium whose swimming behavior is influenced by light. Comprehensive reviews on this subject are available (Petracchi et al., 1994; Oesterhelt and Marwan, 1990; Spudich and Bogomolni, 1988). Marwan et al. (1988) analyzed the photophobic response of H. halobium to dim blue-green flashes. The Poisson curve for a single photon fitted their experimental data well (frequency of reversals versus photon fluence). Thus they took this result as evidence that a single photon is enough to excite the transduction-chain signaling from the sensory pigment to the flagellar motor switch.

There are, however, two technical difficulties in supporting this interpretation. The first one was also pointed out by Marwan et al. (1988). Although the Poisson curve for a single photon has the same shape and steepness as the experimentally derived dose-response curve, the absolute α value must be shifted by a factor ranging from 10 to 20 along the x axis. In other words, the experimental data describe a less sensitive response than that of the theoretical curve. A second problem is evident from data obtained on mutants unable to synthesize retinal. In these "blind" mutants, it is possible to restore the normal behavior in response to light stimuli by introducing in the medium the native retinal or its analogs. By varying the chromophore, it is possible to change the lifetime of the activated pigment, as tested by flash-photolysis experiments (Yan et al., 1991a,b; Takahashi et al., 1992). A relevant result of such experiments is that the absolute sensitivity of this sensory system depends on the lifetime of the excited pigment, whereas the slope of the dose-response curves does not (or varies slightly with it). This point has been highlighted by Takahashi et al. (1992). On the other hand, it may be recalled that the shape of the curve and the absolute sensitivity are closely connected in a plain Poisson model.

This gave us the motivation to look for other effects that could contribute to the general understanding of different sets of experimental data. We started by considering that the noise arising from chemical reactions should be relevant when the number of molecules taking part in the process is low ($1 \div 10^2$), as can occur for signaling molecules in a small cell compartment. Because this noise is due to the fact that molecules can be counted as discrete quantities, we call this kind of noise "chemical shot noise" (CSN). To discuss the relevance of CSN, we analyze a simple basic scheme of enzymatic amplification. The existence of an amplifying catalytic step in photoreception is generally accepted both in bacteria and in eukaryotes.

We confine ourselves to analyzing the basic model described below. We could extend this analysis, in particular the computer simulation, to more complex schemes (for instance that used by Forti et al. (1989) in schematizing the visual cascade in rods). However, our present interest is to analyze a simple model, with only a few parameters, to establish criteria for understanding the effects of CSN. We will discuss the following problems: the way in which CSN is generated, its relevance compared with the input shot noise, and how much CSN can increase the output noise when several amplification steps are operating.

In the first section and in the Appendix, we present the mathematical background for the treatment of the noise inherent in phototransduction chains. Then, Monte Carlo simulations are reported for simple schemes of signal amplification, and the effect of CSN on dose-response curves is presented. The disagreement in the results with respect to previous analyses (Borsellino and Fuortes, 1968a,b) is also discussed.

RESULTS OF ANALYTICAL AND SIMULATION STUDIES

Analytical treatment of the starting model

Scheme 1 shows the first step in the transduction chain of archebacterial sensory rhodopsin. This scheme, a widely
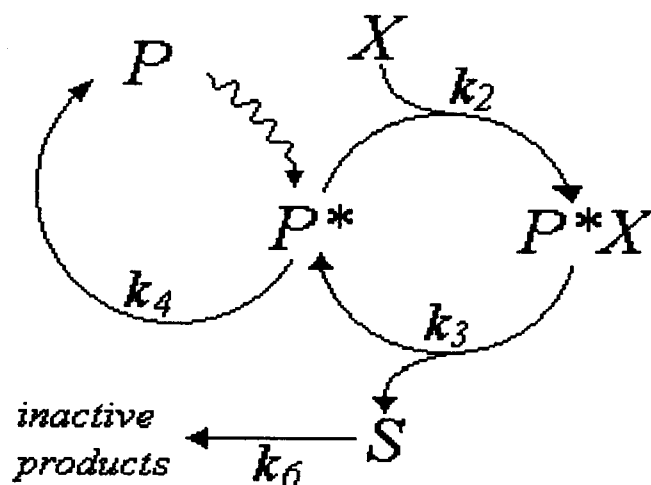
Scheme 1. Minimal kinetic scheme for phototransduction in H. halobium.

accepted hypothesis to account for *H. halobium* photobehavior (Marwan and Oesterhelt, 1987), depicts the activated pigment *P** as a catalyst for a signal-producing reaction. Although we use the time constants of this particular model, formally equivalent schemes can be envisaged for other photoreceptors, such as those of the visual systems of eukaryotes.

We shall now consider in detail what happens when a photon is absorbed. Let us assume $k_2 > k_4$, so that at each time the activated pigment *P** has a greater probability to promote the transformation of *X* in *S* than to decay to *P*. The activated pigment *P** lasts on the average a time k_4^{-1}, assuming $k_3 \gg k_2$. In this way, the time spent by the pigment in the catalytic cycle is negligible with respect to its decay process, and the loop acts simply as an amplifying stage. Note that k_2 is an apparent first-order rate constant, containing the concentration of *X*, whose amount is in excess of *P** under the condition of low stimulation. Because $k_3 \gg k_2$, the probability density function of the actual lifetime of *P** is given by the following equation (Petracchi et al., 1994):

$$f(t) = k_4 e^{-k_4 t} \qquad (3)$$

Thus, $f(t)dt$ is the probability that *P** decays between *t* and *dt*.

In Scheme 1, *S* is the signaling factor, or transducer, acting on some effector; *X* is the precursor of *S*. We may think that the number of *S* molecules ever produced must cross a threshold in order to elicit a response. We initially

will assume that *S* accumulates indefinitely. This is by no means a realistic feature, but we shall deal later with the decay of the signal molecule. The introduction of the threshold mechanism is required when dealing with perceptive or behavioral responses. To emphasize the role of noise in the transduction stages, we adopt a sharp (or stable) threshold criterion at the behavioral output of the system. The definition of threshold stated above could be changed (for instance, the number of *S* molecules existing at any time), and we found that this produced little change in the results.

The problem is now to evaluate how many molecules of *S* are formed per *P** molecule. If the activated pigment lasts a time *t*, $k_2 t$ molecules of *S* are formed on the average, k_2 being the probability per unit time that an *S* molecule is formed. The probability that an activated pigment molecule, lasting *t* seconds in the activated state, generates *n* molecules of *S* is therefore given by:

$$P_1(n, t) = \frac{(k_2 t)^n}{n!} e^{-k_2 t} \qquad (4)$$

$P_1(n, t)$ means probability of formation of *n* molecules within *t* after the absorption of a single photon under the condition that the activated pigment lasts a time *t*. In order to include all possible *t* values, we must combine Eq. 4 with the probability of the actual lifetime *t* for the activated pigment whose probability density function is $f(t) = k_4 e^{-k_4 t}$. The result is:

$$P_1(n) = \int_0^\infty \frac{(k_2 t)^n}{n!} e^{-k_2 t} k_4 e^{-k_4 t} dt$$

and since $\int_0^\infty x^n e^{-x} dx = n!$, by putting $x = (k_2 + k_4)t$ we finally get

$$P_1(n) = q^n (1 - q) \qquad (5)$$

where $q = k_2/(k_2 + k_4)$. This is the same probability function ("discrete exponential") used by Grzywacz and Hillman (1985) in their linear chain model devised to test the linearity of photoreceptor transduction processes.

$P_1(n)$ is the probability of producing *n* molecules of the transducer *S* when a single photon is absorbed. From Eq. 5, we obtain the average number of *S* molecules, which is the amplifying factor of the loop:

$$\bar{n}_1 = \frac{k_2}{k_4} = G \qquad (6)$$

The variance of *n* also comes from Eq. 5:

$$\sigma_1^2 = \overline{(n - \bar{n}_1)^2} = \bar{n}_1 (\bar{n}_1 + 1) \qquad (7)$$

When two photons are absorbed, the probability that *n* molecules of *S* are formed arises from all the possible ways

in which complementary fractions of n are distributed among the two photons:

$$P_2(n) = \sum_{l=0}^{n} P_1(l)P_1(n - l) = \sum_{l=0}^{n} q^l q^{n-l}(1 - q)^2$$

$$= (n + 1)q^n(1 - q)^2 \tag{8}$$

By iteration, in the case that m photons are absorbed, we get the general result:

$$P_m(n) = q^n (1 - q)^m \frac{(n + 1)(n + 2)\ldots(n + m - 1)}{(m - 1)!} \tag{9}$$

Because the system is linear, $\bar{n}_m = m \times \bar{n}_1$ and the standard deviation of n_m is $\sigma_m = \sqrt{m} \times \sigma_1$. This variability in the number of S molecules is due completely to the transduction process, because m is a fixed number. A simple numerical example may help to make this point clear: for $m = 10$ and $n_1 = 10$, we get $n_{10} = 100$, with SD $\sigma_m \approx 33$. This noise is quite relevant. The variation coefficient (defined as the ratio of the standard deviation to the mean) is the same as that of the activated pigment number when 10 photons on average are absorbed, because the standard deviation of a Poisson process is the square root of the mean.

The following question was then considered: Is CSN relevant when compared with the input noise? To answer this, we carried out the computation of the standard deviation expected when α photons on average are absorbed, by combining σ_m with the Poisson law (see Appendix A). Obviously, we have $n_\alpha = G \alpha$, whereas for the standard deviation we obtain, for high gain:

$$\sigma \cong \sqrt{2G^2\alpha} \tag{10}$$

Equation 10 tells us that at the output of the enzymatic loop the variation coefficient (ratio between the standard deviation and the mean) is increased by the factor $2^{1/2}$ when compared with the input, thus showing that CSN is not negligible. This holds for high values of G; when the gain is low, the increase in the variation coefficient is higher than $2^{1/2}$ (see Appendix A, Eq. A5).

Computer simulations on the starting model

To get an intuitive vision of the behavior of the model in Scheme 1, we carried out computer simulations. A finite time constant (k_6) for the decay of S was introduced as a more realistic feature. The differential equations describing the macroscopic behavior of this system (see Scheme 1) are

$$\frac{d[P^*]}{dt} = k_3[P^* X] - (k_2 + k_4)[P^*]$$

$$\frac{d[P^* X]}{dt} = k_2[P^*] - k_3[P^* X] \tag{11}$$

$$\frac{d[S]}{dt} = k_3[P^* X] - k_6[S]$$

Because of the linear structure of the system, Eq. 11 also give its average behavior when the number of involved molecules is low (Borsellino and Fuortes, 1968a).

At the microscopic level, it is important to realize that each chemical transformation is a probabilistic process; therefore, in the simulations, the rate constants of the scheme are used as the probability densities of transition for the corresponding species (for each single molecule). Simulations are performed step by step, and a time interval Δt much shorter than the shortest time constant in the scheme is chosen. In this way, $k_n \Delta t \ll 1$ can be used as a probability. At each step, a random number (uniformly distributed in the range $0 \div 1$) is generated; each molecule of each chemical species can either undergo a transition or remain in its original state, according to whether the random number is in the range $k_n \Delta t$.

Fig. 1 A shows the raw traces of the time course of S in the case that a fixed number of photons are absorbed by the cell; the noise in the output is entirely due to CSN. In Fig. 1 B, we report the average and standard deviation of 100 trials obtained with the same parameters as in Fig. 1 A. By setting $k_6 = 0$ (no decay of S molecules), the standard deviation of simulated data agrees perfectly with Eq. 7, which is a test of the simulation.

The standard deviation reported in Fig. 1 B varies with time and also differs at two time values corresponding to identical values of the mean, a result at variance with the prediction of Borsellino and Fuortes (1968a). This point deserves a detailed discussion. In their fundamental paper, Borsellino and Fuortes (1968a) were looking for a general expression for the probability of having n molecules of transducer at time t upon the absorption of a single photon. They obtained the following result:

$$P(n, t) = \frac{m(t)^n}{n!} e^{-m(t)} \tag{12}$$

(Equation 12 is a copy of Eq. 28A in Borsellino and Fuortes (1968a), with slight changes of symbols.) Although this result has been shown to be incorrect (Goldring and Lisman, 1983), the Borsellino-Fuortes model is still considered valid. In this equation, the first member is the probability of having n molecules at time t (after an arbitrary number of amplifying steps), whereas $m(t)$ is the average number expected at time t. Equation 12 states that the distribution of the number of molecules during a chemical amplification is a Poisson distribution and implies that the standard deviation is at each time t the square root of the average number expected at that time, so that the higher the amplification, the lower the variation coefficient.

On the other hand, our Eq. 7, which holds for an infinite decay time, states that upon the absorption of a single photon the variation coefficient cannot be lower than the mean, whatever the amplification factor may be. As stated above, the simulation with $k_6 = 0$ perfectly agrees with the prediction of Eq. 7. Fig. 2 reports the mean and standard deviation of 100 raw traces in the case that one photon is
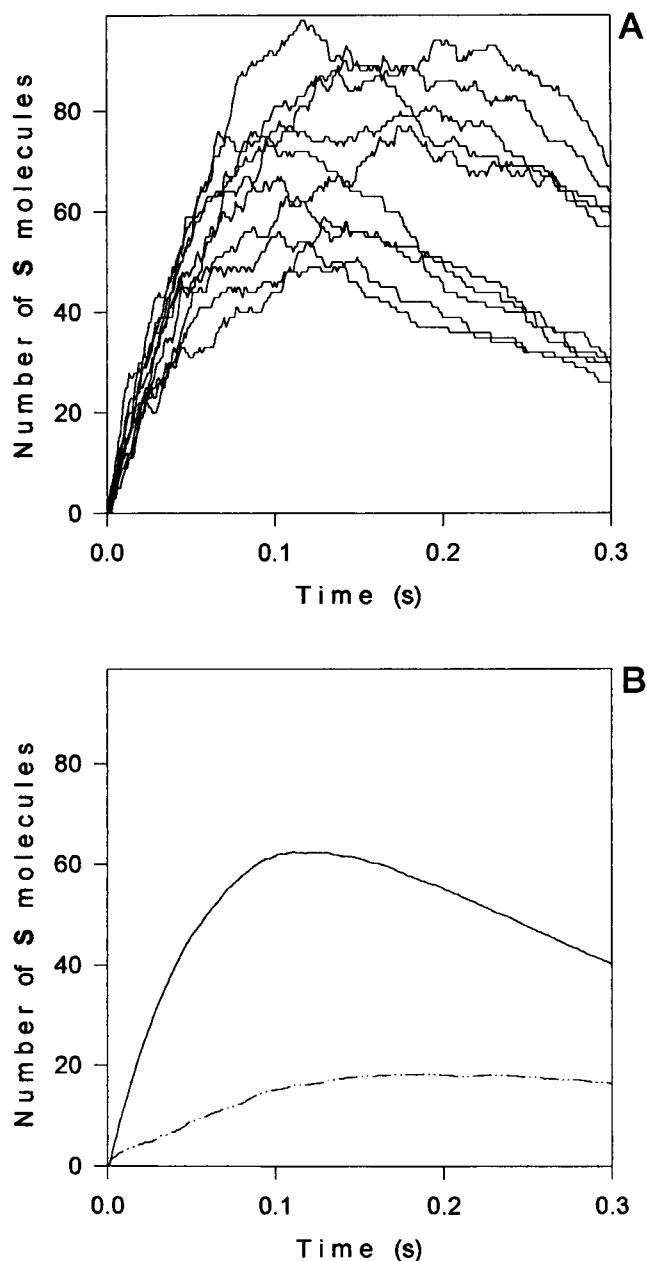
A

B

FIGURE 1   (A) Simulated time courses for the number of S molecules upon the absorption of 10 photons; k_2 = 143 s^{-1}; k_4 = 14.3 s^{-1}; k_6 = 3 s^{-1}. Ten raw traces are reported. (B) The mean (*solid line*) and standard deviation (*dashed line*) of 100 raw traces obtained as in A are reported.

FIGURE 2   The mean (*solid line*) and standard deviation (*dashed line*) of 100 raw traces obtained with the same parameters as those of Fig. 1 upon the absorption of a single photon. The dotted line is the standard deviation expected from Eq. 28A of Borsellino and Fuortes (1968a).

absorbed. The standard deviation derived from Eq. 12, displayed by the dotted line in Fig. 2, is the square root of the mean and is far different from the simulated value. Note also that the standard deviation according to Borsellino and Fuortes (1968a) takes on the same value for equal values of the average on both the increasing and the decreasing part of the time course, which does not occur in the simulation. The correct equation obtained by Goldring and Lisman (1983) (instead of Eq. 12) is too cumbersome, however, to be used straightforwardly. We therefore adopted Eq. 7 in the fol-
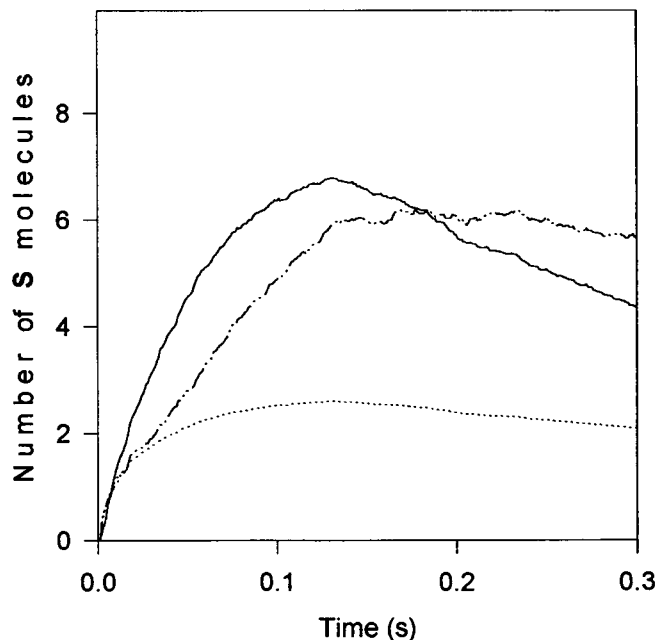
lowing treatment of the transduction model and accordingly used the accumulation value of S molecules.

In a real experiment, the actual number of absorbed photons fluctuates randomly according to Poisson statistics. Fig. 3 reports the results from simulations in which the number of actually absorbed photons in each run was randomly selected according to Poisson distribution. One hundred trials were performed, with an average number of 10 absorbed photons and a 10-fold gain, and their standard deviation is displayed by the solid line. The dashed lines in Fig. 3 are obtained through Eq. 11, fed with any number of photons (i.e., P^* molecules). The resulting curves, each multiplied by their Poisson weight to take into account the input noise, were then averaged, and their standard deviation was computed accordingly. Because of the linear structure of the system, the mean value of the simulation (not shown in Fig. 3) practically coincides with that of the analytical solution of Eq. 11, but its standard deviation is always higher than that obtained by the analytical solution. Therefore, the noise intrinsic to chemical transduction actually contributes to the output noise. The simulated standard deviation, at its maximum in Fig. 3, is 1.4 ($\approx 2^{1/2}$) times higher than that because of the input noise alone (curve (b)), in fairly good agreement with Eq. 10, although this equation was derived for an accumulating product.

Interpretation of dose-response curves

Now let us come back to the meaning of Eq. 9. Clearly, what is important is the number of S molecules produced,
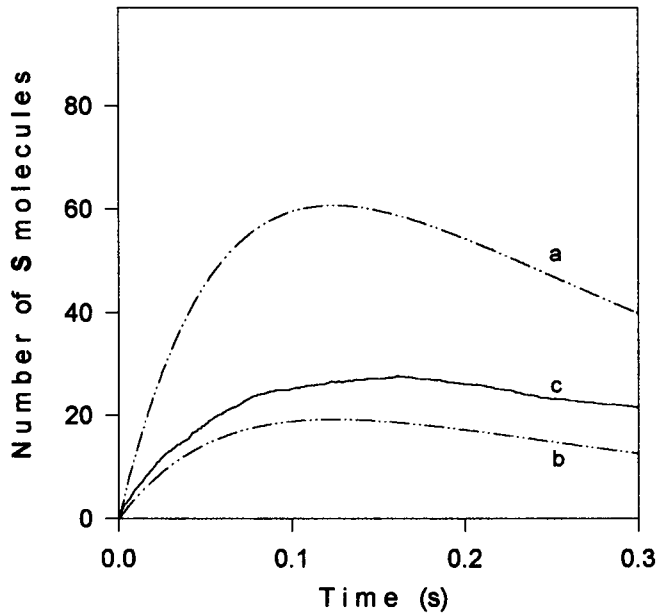
FIGURE 3   Time course of mean value and standard deviation of S molecules produced by simulation with an average number of 10 absorbed photons. Dashed lines are the mean (a) and standard deviation (b) calculated from the analytical solution of Eq. 11; the solid line (c) is the standard deviation for 100 raw traces obtained by Monte Carlo simulation. The mean values of the simulation (not shown) practically coincide with that of the analytical solution.

not the number of photons that actually produced them. Equation 9 states that the same number of S molecules can be produced (with different probabilities) by different numbers of photons, as can readily be appreciated from Fig. 4.
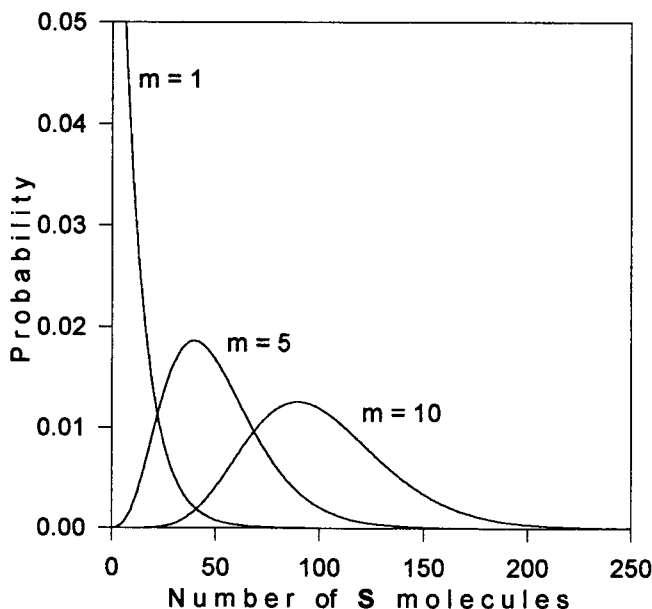

FIGURE 4   Probability that a certain number of S molecules are produced after the absorption of a fixed number of photons (m); the amplification factor is 10.

Therefore, until now the question about the interpretation of dose-response curves has been conceptually incorrect, and we shall reshape it as follows.

When a dim light flash is delivered on a cell population, different numbers of photons will be absorbed by each cell. Let us assume that a sharp threshold criterion holds for the response to occur. Upon the absorption of a fixed number of photons (m), the response arises when the number (n) of S molecules crosses a threshold value X. Then, the probability of response $P_{resp}(m)$ is given by

$$P_{resp}(m) = \sum_{n=X}^{\infty} q^n (1 - q)^m \frac{(n + 1)(n + 2)...(n + m - 1)}{(m - 1)!}$$

(13)

In the bar diagram of Fig. 5, each bar represents a fraction of the cell population (total $= 1$) according to the number of photons (m) actually absorbed (the number below each bar), with $\alpha = 1$. The probability of response calculated from Eq. 13, with $q = 0.91$ ($k_2/k_4 = 10$), is used to evaluate the percentage of cells that do respond to the light flash (*black area in each bar* of Fig. 5).

It is evident that Eq. 13 cannot be used directly to analyze experimental data when the actual number of absorbed photons by any single cell is unknown. In order to adopt α as a measure of stimulus intensity, Eq. 13 has to be combined with the Poisson expression (1) to give

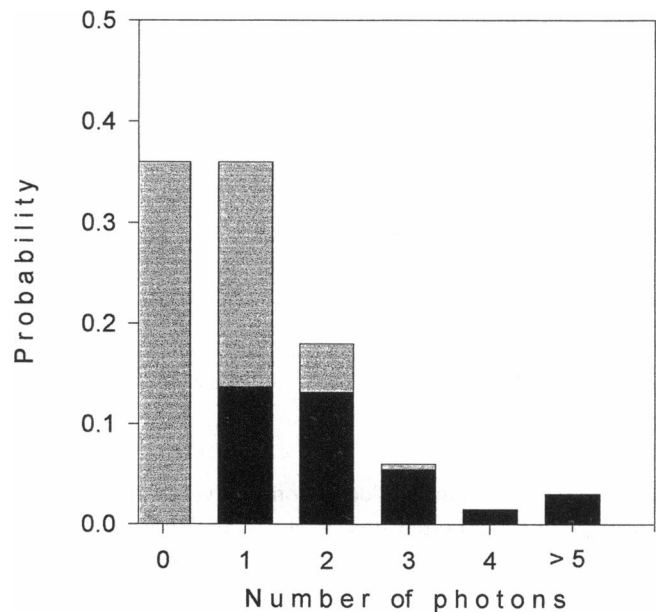$$F_{resp}(\alpha) = \sum_{m=1}^{\infty} P_{resp}(m) \frac{\alpha^m}{m!} e^{-\alpha}$$

(14)

FIGURE 5   Bar diagram illustrating the percentage of responding cells after the absorption of different numbers of photons; $k_2/k_4 = 10$, $\alpha = 1$, $X = 10$. The numbers below each bar are the photons actually absorbed by that percentage (= height of the bar) of cells; the fraction of responding cells in each bar is shown by the black shading, whereas the hatched area shows the fraction of cells that do not respond.

Now, $F_{resp}(\alpha)$ and α can be experimentally determined and $P_{resp}(m)$ can be calculated, thus allowing the use of Eq. 14 to fit curves to experimental data. Fig. 6 reports three dose-response curves computed according to Eq. 14 with different X values; the steepness of these curves increases with the value of X. The curve on the left is nearly as steep as that from Eq. 1 with $l = 1$, but it is shifted along the x axis by a factor of ~3. The shift for the *H. halobium* dose-response curves was found experimentally to be nearly 10 (Marwan et al., 1988). However, we could not obtain a higher shift even though many different values were used for the kinetic parameters of the model.

Models with a cascade of amplifying loops

The results of the preceding section have shown that when phenomena like those observed in *H. halobium* (Marwan et al., 1988) are to be interpreted, the simple model initially considered cannot account quantitatively for the experimentally observed shift. Generally speaking, it is also unusual to find a photoreceptor transduction chain made up of just a single catalytic loop. In this section we therefore want to discuss the effects of CSN in a receptor system when a more general scheme with a cascade of (linear) amplifying loops is assumed.

In Appendix B, we derive expression (B3) for the standard deviation of the final product S of the amplifying cascade. Let us discuss here briefly the meaning of expres-

sion (B3), which for identical loops with the same amplification factor becomes

$$\sigma_k^2 = G^{2k} \alpha \left(2 \sum_{l=0}^{k-1} \frac{1}{G^l} + \frac{1}{G^k} \right) \qquad (15)$$

The qualitative behavior of the system is not changed by introducing several amplifying loops in the cascade, provided the amplification factor of each stage is substantially greater than one. Responses to a single photon still have an exponential distribution, as shown also by Grzywacz and Hillman (1985) and by Goldring and Lisman (1994), and the ratio of the standard deviation to the mean changes little from that arising from the first loop, as the contribution of $1/G$ and its powers is small.

When G is low at every step and considerable amplification arises only after many steps, however, a noticeable increase in the standard deviation occurs. This is best shown by considering an overall value of $G = 10$. When this value is obtained in a single step, the output has a $\sigma = 1.45G\sqrt{\alpha}$, whereas when it is obtained in 10 steps, each with $G = 1.26$ (and $1.26^{10} \approx 10$), one gets $\sigma = 2.97G^{10}\sqrt{\alpha}$. Once again our results differ from those of Borsellino and Fuortes (1968a,b). The standard deviation coming out of Eq. 28A in Borsellino and Fuortes (1968a) is the square root of the average and consequently does not depend on the number of amplifying stages or on their order. It depends only on the overall amplification.

A low amplification factor implies a considerable probability that the catalyst of a chemical step decays to the inactive state before ever producing a single molecule of transducer (failure in molecular amplification). This phenomenon, discussed by Grzywacz and Hillman (1985) and thoroughly investigated by Goldring and Lisman (1994), could account for the shift in sensitivity of the dose-response curve in *H. halobium* and provide an interpretation at the molecular level of the low photon yield found by Marwan et al. (1988). By the same token, when the first few steps in the cascade do not amplify ($G = 1$) and are followed by an amplifying step, a similar effect on the dose-response curve is expected. This type of cascade was adopted by Goldring and Lisman (1983) in a simulation of quantum bump kinetics of the *Limulus* ventral receptors. However, we must take into account that changing the time constants of the pigment photocycle produces a shift in the experimental dose-response curves without affecting their slope (Takahashi et al., 1992). We therefore had to find what out happens in the model when the gain in the first step is changed.

We found that the increase of noise in a chain of amplifying loops with a low amplification per loop, predicted by Eq. 15, affects the dose-response curves, and it becomes possible to obtain dose-response curves overlapping to Eq. 1 with $l = 1$ but shifted on the α axis by a factor of 10, as shown in Fig. 7. This curve has been obtained by simulating a 10-step transduction chain, each step having $G = 1.26$, fed
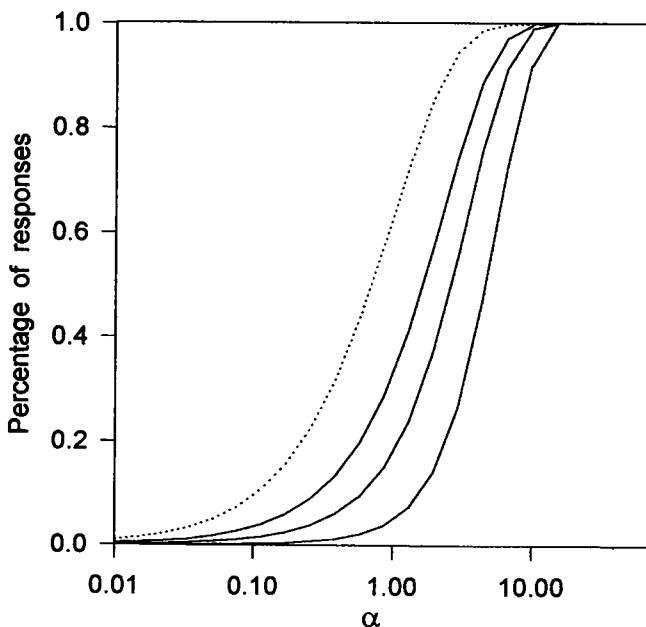

FIGURE 6   Computed dose-response curves for a photosensory-effector system with $G = k_2/k_4 = 10$. The probability of the response is plotted against log α. The three curves (*solid lines*) differ for the threshold value: left curve, $X = 10$; middle curve, $X = 20$; right curve, $X = 40$. The dotted line is a Poisson curve with $l = 1$.
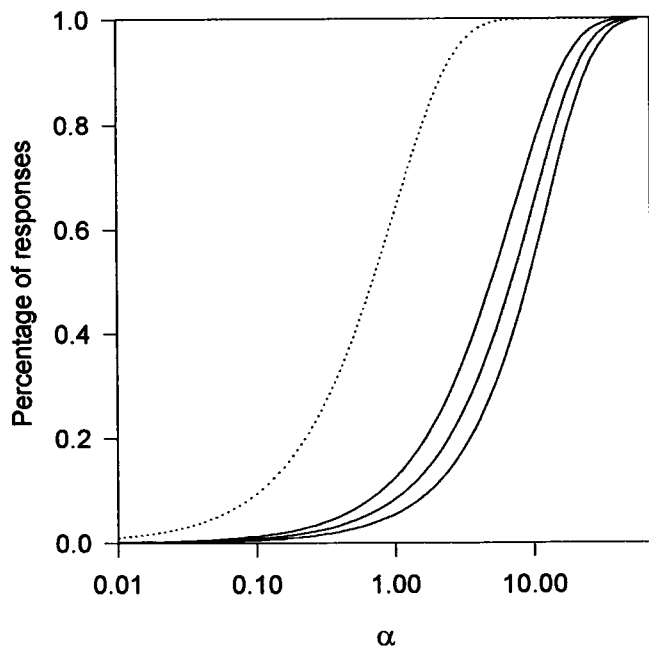
FIGURE 7   Computed dose-response curves for a photosensory-effector system acting through 10 low-amplifying loops in cascade. In each amplifying step, $G = 1.26$. The three curves (*solid lines*) differ for the threshold value: left curve, $X = 10$; middle curve, $X = 20$; right curve, $X = 30$. The dotted line is a Poisson curve with $l = 1$.

with 1, 2, 3 ... m photons. A threshold criterion on the output of the cascade was used to evaluate the probabilities of response as a function of m. These probabilities were eventually combined with the Poisson law according to Eq. 14 to obtain the dose-response curve. By adopting this kind of scheme, it is possible to account for the relevant features of experimental dose-response curves for the motile photobehavior of *H. halobium* (Marwan et al., 1988; Takahashi et al., 1992). When the threshold is kept constant and the value of G of the first step is increased, the simulated curve is shifted to the left and coincides with a true Poisson curve with $l = 1$ (not shown), in agreement with the experimental data cited above.

Ten stages may seem to be too many. Similar results could be obtained with fewer stages (for instance, five) by setting to one the gain of the first three to four stages, amplification arising from the last stage; the first stage becomes amplifying when the pigment is changed (results not shown).

DISCUSSION

In devising the basic model to investigate the general properties outlined here, we aimed to include the minimal features of a sensory-effector transduction system. Therefore, the outcomes of this study are to be considered as fundamental properties of any such system, and a real sensory system should be compared with the properties of this basic

model before any *ad hoc* hypothesis is introduced to explain its behavior.

At present we can put forth some general remarks on sensory transduction through enzymatic amplification processes by summarizing the results reported above, as well as those of other authors, in the following points. 1) The amount of transmitter produced upon the absorption of a few photons is not fixed but varies stochastically. In particular, an exponential distribution of the whole amount of transmitter produced upon the absorption of a single photon is expected (see also Kirkwood and Lisman (1994) and Grzywacz and Hillman (1985)). 2) Because the standard deviation of exponential distribution is equal to the mean, appreciable noise arises from the fluctuations because of a single-step enzyme amplification, and this shot noise is comparable to the input noise; the output variation coefficient increases, with respect to the input noise, by a factor $\approx \sqrt{2}$ for a single amplifying loop with large gain. 3) CSN in a single amplifying step can partially account for the discrepancy between experimental dose-response curves in *H. halobium* and the Poisson single-photon curve, because the variability intrinsic to chemical amplification can generate a lower absolute sensitivity, but not so low as to yield a 10- to 20-fold shift along the α axis. A cascade of low-gain amplifying loops could account instead for shifts of the same order as those experimentally observed.

The point that we want to stress is that the currently accepted interpretation of fluence-response curves (of *H. halobium* and perhaps of human perception) in terms of the minimum number of photons required to elicit a response should be reformulated considering the probabilities that 1, 2, 3, ... n photons will give rise to a sensation or a change in behavior. An attempt in this direction was made in modeling the *H. halobium* dose-response curves (Takahashi et al., 1992) by making the overall "quantum yield" of the transduction process a (nonlinear) function of the number of actually absorbed photons. We show that nonlinear steps in the amplifying cascade are not required to reformulate the problem of photon requirement in probabilistic terms, because an answer to this problem simply comes out of basic statistical causes, independently of the details in the transduction process. Molecular failure in transduction, when the amplification factor is low, can thus account for the lower sensitivity of the system and for the intuitive interpretation that just 1 out of 10-20 activated pigment molecules have success in reversing the motion (Marwan et al., 1988). A quantitative fitting of the present models to experimental data should await the acquisition of more details (e.g., amplification coefficient for the first stage) on the real transduction system of *H. halobium*.

APPENDIX A

Calculation of the standard deviation for the responses elicited when flashes of α average photon fluence are delivered on a photosensitive sample

As observed in the text, because the system is linear, the responses to m photons are given by the sum of m responses to a single photon. Thus, the average number of signaling molecules produced by m photons is $\bar{n}_m = m\bar{n}_1 = mG$, and the standard deviation $\sigma_m = \sigma_1 \sqrt{m} = \sqrt{m} \sqrt{G(G+1)}$.

Consider now a real experiment in which flashes of constant average energy α are delivered on a photosensitive sample. The actual number of absorbed photons will be distributed according to Eq. 1. Because the system is linear, we will have $\bar{n}_\alpha = G\alpha$. A set of N trials can be divided into subsets I_m, on the basis of the number m of actually activated photoreceptors. Let $N(m)$ be the number of trials belonging to I_m; then, where $P_{pois}(m)$ is given by Eq. 1 in the text. We want now to obtain an expression for the variance relative to the general average $\bar{n}_\alpha = G\alpha$. By definition, the variance is given by

$$\sigma^2 = \sum_{J=1}^{N} \frac{(n_J - G\alpha)^2}{N} \qquad (A1)$$

and we can write it as

$$\sigma^2 = \sum_m \sigma_{I_m}^2 P_{pois}(m) \qquad (A2)$$

where $\sigma_{I_m}^2$ is the contribution to the variance from subset I_m.

Let $n_{i,m}$ be the actual number of S molecules produced in the ith trial (flash) belonging to the I_m subset. In this subset, the average number of S molecules is Gm, and the local variance is $G^2 m$. The variance relative to the general average $G\alpha$ is

$$\sigma_{I_m}^2 = \sum_{i=1}^{N(m)} \frac{[(n_{i,m} - Gm) + G(m - \alpha)]^2}{N(m)}$$

$$= G^2(m - \alpha)^2 + \sum_{i=1}^{N(m)} \frac{(n_{i,m} - Gm)^2}{N(m)} \qquad (A3)$$

The last term on the right in Eq. A3 is the local variance $\sigma_m^2 = G^2 m$, thence we can rewrite Eq. A2 as

$$\sigma^2 = \sum_m [G^2(m - \alpha)^2 + G^2 m + Gm] P_{pois}(m) \qquad (A4)$$

and finally

$$\sigma^2 = G^2 \sigma_{pois} + G^2 \alpha + G\alpha = 2G^2 \alpha + G\alpha \qquad (A5)$$

Equation A5 means that the output noise after a transduction step is actually increased over the input noise. The variation coefficient (standard deviation/mean value) is $\geq \sqrt{2/\alpha}$ in the output, where the equal sign holds for high gain. Since $1/\sqrt{\alpha}$ is the same ratio in the input, the output variation coefficient is increased at least by the factor $\sqrt{2}$ after a single amplification step, so that the signal-to-noise ratio is decreased by the same amount.

APPENDIX B

Calculation of the standard deviation in the output of a multi-step amplifying cascade

In deriving this result, we assume that a signal molecule is produced after a number of steps consisting of catalytic amplifying loops and that this molecule does not decay. We are interested in the number of molecules that accumulate after a dim flash, its mean and variance.

Consider an amplifying chain of n steps. Equation A4 can in general be written as follows:

$$\sigma_k^2 = \sum_0^{\infty} [G_k^2 (m - \bar{m})^2 + G_k^2 m + G_k m] P_{k-1}(m) \qquad (B1)$$

where G_k is the gain of the step k, $\bar{m}$ is the mean value of the number of molecules produced at the step k-1, m is the number of molecules at the step k-1 in each single trial, and $P_{k-1}(m)$ is the probability of m. Equation A5 is now substituted by

$$\sigma_k^2 = G_k^2 (\bar{m}_{k-1} + \sigma_{k-1}^2) + G_k \bar{m}_{k-1} \qquad (B2)$$

with $k \geq 1$.

From Eq. B2, by iteration and remembering that the input obeys Poisson statistics, one gets:

$$\sigma_0^2 = \alpha \qquad ; \qquad \bar{m}_0 = \alpha$$

$$\sigma_1^2 = G_1^2 (\alpha + \alpha) + G_1 \alpha \qquad ; \qquad \bar{m}_1 = G_1 \alpha$$

$$\sigma_2^2 = G_2^2 G_1^2 \alpha \left(2 + \frac{2}{G_1} + \frac{1}{G_1 G_2}\right) \qquad ; \qquad \bar{m}_2 = G_1 G_2 \alpha \qquad (B3)$$

$$\ldots \ldots \ldots \ldots \ldots \ldots \ldots \ldots \qquad ; \qquad \ldots \ldots \ldots \ldots \ldots \ldots$$

$$\sigma_k^2 = P_k^2 \alpha \left(2 \sum_{l=0}^{k-1} \frac{1}{P_l} + \frac{1}{P_k}\right) \qquad ; \qquad \bar{m}_k = P_k \alpha$$

where $G_0 = 1$ and $P_k = \prod_{j=0}^{k} G_j$.

Equation B3 states that the output variance after n steps does not depend solely on the mean. Moreover, when an overall amplification P is reached through two steps with respective amplifications G_1 and G_2, the sequence of these two steps (i.e., which one precedes the other) may be relevant. For $G_1 > G_2$, the output noise is lower, which is highly plausible and predictable but is in striking disagreement with the equation derived by Borsellino and Fuortes (1968a,b).

REFERENCES

Baylor, D. A., B. J. Nunn, and J. L. Schnapf. 1984. The photocurrent, noise and spectral sensitivity of rods of the monkey *Macaca fascicularis*. *J. Physiol. (Lond.)*. 357:575–607.

Borsellino, A., and M. G. F. Fuortes. 1968a. Responses to single photons in visual cells of *Limulus*. *J. Physiol. (Lond.)*. 196:507–539.

Borsellino, A., and M. G. F. Fuortes. 1968b. Interpretation of responses of visual cells of *Limulus*. *Proc. IEEE*. 56:1024–1032.

Forti, S., A. Menini, G. Rispoli, and V. Torre. 1989. Kinetics of photo-transduction in retinal rods of the newt *Triturus cristatus*. *J. Physiol. (Lond.)*. 419:265–295.

Fuortes, G., and S. Yeandle. 1964. Probability of occurrence of discrete potential waves in the eye of *Limulus*. *J. Gen. Physiol.* 47:443–463.

Goldring, M. A., and J. E. Lisman. 1983. Single photon transduction in *Limulus* photoreceptors and the Borsellino-Fuortes model. *IEEE Trans. on Systems, Man, Cybernetics SMC.* 13:727–731.

Goldring, M. A., and J. E. Lisman. 1994. Multi-step rhodopsin inactivation scheme can account for the size variability of single photon responses in *Limulus* ventral receptors. *J. Gen. Physiol.* 103:691–726.

Grzywacz, N. M., and P. Hillman. 1985. Statistical test of linearity of photoreceptor transduction process: *Limulus* passes, others fail. *Proc. Natl. Acad. Sci. USA.* 82:232–235.

Hecht, S., S. Shlaer, and M. H. Pirenne. 1942. Energy, quanta and vision. *J. Gen. Physiol.* 25:819–840.

Kirkwood, A., and J. E. Lisman. 1994. Determinants of single photon response variability. *J. Gen. Physiol.* 103:679–690.

Lederhofer, R., J. Schnakenberg, and R. Stieve. 1991. Stochastic treatment of bump latency and temporal overlapping in *Limulus* ventral photoreceptors. *Z. Naturforsch. [C].* 46:291–304.

Lillywhite, P. G., and S. B. Laughlin. 1979. Transducer noise in a photoreceptor. *Nature.* 277:569–572.

Marwan, W., P. Hegemann, and D. Oesterhelt. 1988. Single photon detection by an archaebacterium. *J. Mol. Biol.* 199:663–664.

Marwan, W., and D. Oesterhelt. 1987. Signal formation in the halobacterial photophobic response mediated by a fourth retinal protein (P_{480}). *J. Mol. Biol.* 195:333–342.

Menini, A., C. Picco, and S. Firestein. 1995. Quantal-like current fluctuations induced by odorants in olfactory receptor cells. *Nature.* 373:435–437.

Oesterhelt, D., and W. Marwan. 1990. Signal transduction in *Halobacterium halobium*. *In* Biology of the Chemotactic Response. Society for General Microbiology Symposium, Vol. 46. J. P. Armitage and J. M. Lackie, editors. Cambridge University Press. 219–239.

Petracchi, D., S. Lucia, and G. Cercignani. 1994. Photobehaviour of *Halobacterium halobium*: proposed models for signal transduction and motor switching. *J. Photochem. Photobiol. B. Biol.* 24:75–99.

Spudich, J. L., and R. A. Bogomolni. 1988. Sensory rhodopsin of halobacteria. *Annu. Rev. Biophys. Biophys. Chem.* 17:193–215.

Spudich, J. L., and W. Stoeckenius. 1979. Photosensory and chemosensory behavior of *Halobacterium halobium*. *J. Photobiochem. Photobiophys.* 1:43–53.

Takahashi, T., B. Yan, and J. L. Spudich. 1992. Sensitivity increase in the photophobic response of *Halobacterium halobium* reconstituted with retinal analogs: a novel interpretation for the fluence-response relationship and a kinetic modeling. *Photochem. Photobiol.* 56:1119–1128.

Yan, B., K. Nakanishi, and J. Spudich. 1991a. Mechanism of activation of sensory rhodopsin I: evidence for a steric trigger. *Proc. Natl. Acad. Sci. USA.* 88:9412–9416.

Yan, B., T. Takahashi, R. Johnson, and J. L. Spudich. 1991b. Identification of signaling states of a sensory receptor by modulation of lifetimes of stimulus-induced conformations: the case of sensory rhodopsin II. *Biochemistry.* 30:10686–10692.